



The transitional association between β -amyloid pathology and regional brain atrophy

Philip S. Insel^{a,*}, Niklas Mattsson^{a,b,c}, Michael C. Donohue^{d,e}, R. Scott Mackin^a, Paul S. Aisen^e, Clifford R. Jack, Jr.,^f Leslie M. Shaw^g, John Q. Trojanowski^g, Michael W. Weiner^{a,b}, and the Alzheimer's Disease Neuroimaging Initiative¹

^aDepartment of Veterans Affairs Medical Center, Center for Imaging of Neurodegenerative Diseases, San Francisco, CA, USA

^bDepartment of Radiology and Biomedical Imaging, University of California, San Francisco, CA, USA

^cClinical Neurochemistry Laboratory, Institute of Neuroscience and Physiology, The Sahlgrenska Academy, University of Gothenburg, Mölndal, Sweden

^dDivision of Biostatistics & Bioinformatics, Department of Family & Preventive Medicine, University of California, San Diego, CA, USA

^eDepartment of Neurosciences, University of California, San Diego, CA, USA

^fDepartment of Radiology, Mayo Clinic, Rochester, MN, USA

^gDepartment of Pathology and Laboratory Medicine, Institute on Aging, Center for Neurodegenerative Disease Research, University of Pennsylvania School of Medicine, Philadelphia, PA, USA

Abstract

Background: Alzheimer's disease (AD) is characterized by the accumulation of β -amyloid (A β) associated with brain atrophy and cognitive decline. The functional form to model the association between A β and regional brain atrophy has not been well defined. To determine the relationship between A β and atrophy, we compared the performance of the usual dichotomization of cerebrospinal fluid (CSF) A β to identify subjects as A β + and A β - with a trilinear spline model of CSF A β .

Methods: One hundred and eighty-three subjects with mild cognitive impairment and 108 cognitively normal controls with baseline CSF A β and up to 4 years of longitudinal magnetic resonance imaging data from the Alzheimer's Disease Neuroimaging Initiative were analyzed using mixed-effects regression. Piecewise-linear splines were used to evaluate the nonlinear nature of the association between CSF A β and regional atrophy and to identify points of acceleration of atrophy with respect to A β . Several parameterizations of CSF A β were compared using likelihood ratio tests and the Akaike information criterion. Periods of acceleration of atrophy in which subjects transition from CSF A β negativity to CSF A β positivity were estimated from the spline models and tested for significance.

Results: Spline models resulted in better fits for many temporal and parietal regions compared with the dichotomous models. The trilinear model showed that periods of acceleration of atrophy varied greatly by region with early changes seen in the insula, amygdala, precuneus, hippocampus, and other temporal regions, occurring before the clinical threshold for CSF A β positivity.

Conclusion: The use of piecewise-linear splines provides an improved model of the nonlinear association between CSF A β and regional atrophy in regions implicated in the progression of AD. The important biological finding of this work is that some brain regions show periods of accelerated volume loss well before the CSF A β ₄₂ threshold. This implies that signs of brain atrophy develop before the current conventional definition of "preclinical AD".

© 2014 The Alzheimer's Association. Published by Elsevier Inc. All rights reserved.

Keywords: Alzheimer's disease; ADNI; Trilinear; Beta amyloid; Atrophy

¹Data used in preparation of this article were obtained from the Alzheimer's Disease Neuroimaging Initiative (ADNI) database (adni.loni.usc.edu). As such, the investigators within the ADNI contributed to the design and implementation of ADNI and/or provided data but did not participate in analysis or writing of this report. A complete listing of ADNI investigators

can be found at: http://adni.loni.usc.edu/wp-content/uploads/how_to_apply/ADNI_Acknowledgement_List.pdf.

*Corresponding author. Tel.: +1-858-652-8480; Fax: +1-415-668-2864.
E-mail address: philipinsel@gmail.com

1. Introduction

The deposition of fibrillar β -amyloid ($A\beta$) and accelerated brain atrophy are central features of the development of Alzheimer's disease (AD) [1,2]. Some hypothesize that pathological $A\beta$ metabolism is an initiating event in AD [3]. This is supported by biomarker data, especially in familial forms of AD, where $A\beta$ accumulation occurs many years before brain atrophy and the onset of cognitive impairment [4–7]. Recent studies of controls and subjects with mild cognitive impairment (MCI) have shown early $A\beta$ -related changes in brain structure to occur in both temporoparietal regions and frontal gyri [8–11] and also the thalamus and putamen in subjects with familial AD [12]. However, although $A\beta$ deposition has been shown to be associated with gray matter atrophy, neither the nature of the association nor the functional form, i.e. the statistical parameterization, to model their relationship has been well characterized. Additionally, rates of change of $A\beta$ biomarkers have been shown to increase as subjects approach the clinical threshold that best distinguishes AD patients from controls and subsequently plateau [13–15]. These higher rates of change near the threshold may contribute to the apparent bimodal distribution of $A\beta$ levels in cross-sectional analyses [8,16,17], which has led to the common categorization of subjects into amyloid positive ($A\beta+$) and amyloid negative ($A\beta-$) groups. However, little is known about how the transition from $A\beta-$ to $A\beta+$ relates to brain atrophy or how to model their association. The primary purpose of this study is to compare several parameterizations of CSF $A\beta$ in an attempt to better understand the progression of atrophy.

Several approaches have been used to study the association of $A\beta$ with brain atrophy. One approach is to assume a linear effect of $A\beta$ on atrophy. This model assumes that changes in the level of $A\beta$ are associated with atrophy in the same way regardless of whether subjects have pathological levels of $A\beta$ or not. Another approach and the most common parameterization of $A\beta$ is to dichotomize the continuous form at a threshold that best differentiates subjects with a diagnosis of probable AD from subjects without cognitive impairment. A common threshold used for CSF $A\beta$ measurements in the Alzheimer's Disease Neuroimaging Initiative (ADNI) is 192 ng/L, derived by comparing autopsy-confirmed AD patients with controls [17]. This parameterization assumes a constant atrophy rate in each group with no transition period between them. While these models' simplicity allow for easy interpretation, they are unlikely to be realistic representations of the $A\beta$ -atrophy relationship. Other methods, designed to model nonlinearity without specifying a parametric form of the curve, such as local regression [18] or smoothing splines [19] have been used in imaging studies to capture nonlinearity in atrophy rates, usually with respect to time or age [20–22]. The increased flexibility of these methods, however, makes the results of the model difficult to summarize and interpret, especially if the goal is to test a formal hypothesis about

the shape of a curve that relates $A\beta$ to brain atrophy. A more effective model will adequately capture nonlinearity while remaining interpretable.

One possibility is to allow a separate slope to be estimated during the transition from atrophy rates at low levels of $A\beta$ through to a plateau in rates at highly pathological levels. Such a plateau or saturation point of atrophy with respect to $A\beta$ accumulation will likely vary by region, as will the point at which acceleration begins. We propose a combination of local regression and piecewise-linear splines to capture the variation of atrophy rates across the spectrum of $A\beta$ levels. The model allows three separate slopes to be estimated, one before a potential transition period when changes in $A\beta$ have minimal or no association with atrophy rates, one during the transition and one after. This model is similar to the trilinear model used in Brooks et al. [23], but applied at the population level rather than the individual level. Parameters for changes in the slope of the association of $A\beta$ with atrophy are easily interpreted and tested for statistical significance. An initial step in the model fitting process uses local regression to guide the selection of knot locations, i.e. points at which the slope may change.

We hypothesize that piecewise-linear splines will adequately characterize the relationship between CSF $A\beta$ and regional brain atrophy while identifying and testing for departures from linearity. For regions that demonstrate changes in atrophy rates across the span of CSF $A\beta$, periods of acceleration and/or saturation will be identified via the selection of spline knot locations. Knot locations will be taken as data-driven estimates of the beginning and ending of the period of transition. The estimation of these transition periods may be important in the optimization of clinical trials for therapies aimed at reducing $A\beta$ -related atrophy.

2. Methods

2.1. Participants

Data were obtained from the ADNI database (adni.loni.usc.edu). ADNI participants were recruited from over 50 sites across the United States and Canada (see www.adni-info.org). The population in this study included ADNI-1 participants who were classified as healthy controls or mild cognitive impairment (MCI) subjects at ADNI screening, who were tested for CSF $A\beta_{42}$, and who had successful longitudinal FreeSurfer processing of MR images.

2.2. CSF biomarker concentrations

A CSF sample was collected at study baseline by lumbar puncture. CSF $A\beta_{42}$ was measured using the multiplex xMAP Luminex platform (Luminex Corp, Austin, TX) with the Research Use Only INNOBIA AlzBio3 kit (Fujirebio/Innogenetics, Ghent, Belgium) [17,24].

2.3. MRI acquisition and processing

At each site, the subjects underwent the standardized 1.5 T MRI protocol of ADNI, as described in Jack et al. [25]. For more detail, see the “MRI acquisition and processing” section of the [Supplemental Material](#), available online.

2.4. Statistical analysis

Baseline associations between CSF A β_{42} and demographic/clinical factors were assessed using Wilcoxon tests for categorical variables (gender, APOE $\epsilon 4$ positivity) and Spearman correlation for continuous variables (age, education, ADAS-cog). Baseline associations were compared within and across diagnostic groups.

Up to 4 years of repeated measures of 47 regional volumes of gray matter were averaged over right and left hemispheres. The estimation of the association between CSF A β_{42} and atrophy in each of the 47 regions, and global atrophy, was done in two steps. In the first step, longitudinal volumes were regressed on time since baseline scan using mixed effects regression. All models included both a random intercept and slope. In a second step, subject-specific slopes from the mixed model were then regressed on baseline CSF A β_{42} level, adjusting for age and gender, using ordinary least squares regression. In the second regression, the effect of CSF A β_{42} was modeled using three line segments, separated by two spline knots to allow for departures from linearity.

To improve the fit of the splines, local regression was used to guide the selection of knot locations. The sparsity of data near the clinical threshold of CSF A β_{42} = 192 ng/L appeared problematic and resulted in poor fits when knot locations were selected without an intermediate local regression step. The estimation of the local regression curve depends on a weighted function of a neighborhood of points in the predictor, CSF A β_{42} . The specification of this neighborhood determines the smoothness of the curve and the degree to which it is robust to outliers and sparsity in the data. The level of smoothness of the local regressions was determined via 10-fold cross-validation to minimize residual error. Knot locations were then identified by regressing the estimated values for atrophy from the local regression on

CSF A β , while allowing knot locations to vary from 125 to 250 ng/L. For each region, locations were chosen to maximize agreement with local regression fits. Models were then refit with splines and selected knot locations.

Steps 1 and 2 were repeated in 500 bootstrap samples to estimate confidence intervals for the association of CSF A β_{42} with atrophy using the 2.5th and 97.5th percentiles. We used the studentized bootstrap [26] with a false discovery rate correction [27] to obtain *P*-values for slopes and test for significance of acceleration/saturation. All tests were two sided. Likelihood ratio tests and AIC were used to compare the spline vs. dichotomous parameterization of CSF A β_{42} . All analyses were done in R v2.12.

3. Results

One hundred and eight controls and 183 MCI subjects had both CSF and longitudinal structural MRI data and were included in the analysis. The median number of scans for both controls and MCI subjects was 5, with 291 scans (baseline), 282 (month 6), 263 (month 12), 143 (month 18, MCI only), 209 (month 24), 143 (month 36), and 35 (month 48). There were no significant associations between baseline CSF A β_{42} and age, gender, or education (Table 1). CSF A β_{42} was significantly associated with both APOE $\epsilon 4$ positivity and ADAS-cog within both diagnostic groups.

Plots of six regions including both MCI and control subjects are shown in Fig. 1. Regions in the plot were selected to show where the trilinear model appeared to fit well (hippocampus, entorhinal cortex, banks of the superior temporal sulcus, and middle temporal gyrus), one region where the spline and local regression differed, and a control region where the association between CSF A β_{42} and atrophy was weak (pericalcarine). Spline, binary, and local regression curves are shown and 95% confidence intervals for the spline curve. The ability of the spline models to predict atrophy, as measured by cross-validated R², was similar to the predictive ability of the local regression models, with most regions differing by <0.01, and 3 of the 47 regions differing by almost 0.02.

Table 2 shows the knot locations, parameter estimates, *P*-values and false discovery rate (FDR)-corrected *P*-values for each spline segment, for each region that demonstrated at

Table 1
Baseline characteristics

	Controls (N = 108)		MCI (N = 183)		Controls and MCI (N = 291)	
	Mean (SD)	$\rho_{A\beta}$ (<i>P</i>)*	Mean (SD)	$\rho_{A\beta}$ (<i>P</i>)	Mean (SD)	$\rho_{A\beta}$ (<i>P</i>)
CSF A β_{42} , ng/L	204 (55)	–	165 (56)	–	179 (58)	–
Age	75.5 (5.3)	–0.08 (.38)	74.4 (7.2)	0.05 (.49)	74.8 (6.6)	0.02 (.67)
Gender (F)	48%	– (.48) [†]	34%	– (.11)	39%	– (.86)
Education (yrs)	15.8 (2.84)	–0.05 (.61)	15.7 (3.0)	–0.003 (.97)	15.7 (2.9)	–0.01 (.89)
APOE $\epsilon 4$ +	23%	– (<.01) [†]	55%	– (<.01)	43%	– (<.01)
ADAS-cog	6.4 (3.0)	–0.22 (.02)	11.7 (4.6)	–0.20 (<.01)	9.71 (4.79)	0.35 (<.01)

Abbreviations: MCI, mild cognitive impairment; CSF, cerebrospinal fluid; SD, standard deviation; A β , amyloid beta.

*Spearman correlation with A β and corresponding *P*-value.

[†]Wilcoxon rank sum test for A β and corresponding *P*-value.

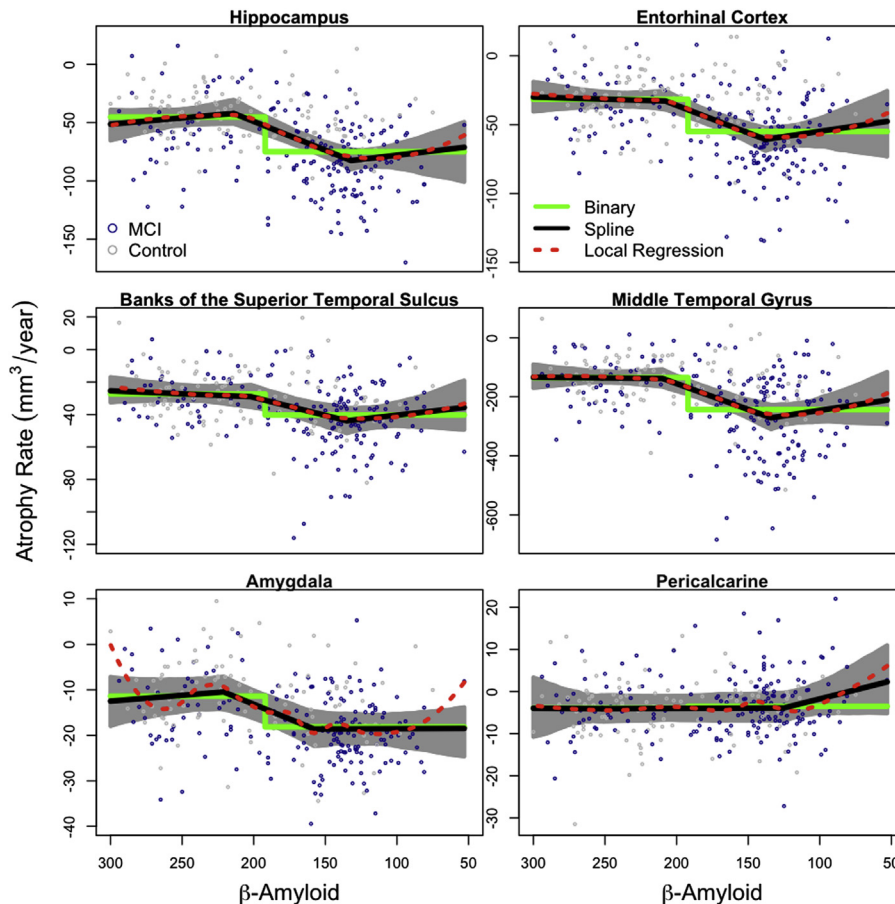


Fig. 1. Atrophy rates of six regions plotted against cerebrospinal fluid (CSF) amyloid beta-42 ($A\beta_{42}$) in mild cognitive impairment (MCI) and control subjects. Note that values on the CSF $A\beta_{42}$ axis go from high (less pathology) on the left to low (more pathology) on the right. Three curves are shown: binary in green, local regression in red, and trilinear spline in black. The shaded region is the 95% confidence interval for the spline curve.

least marginal atrophy acceleration associated with $A\beta_{42}$ ($P < .10$). The parameter estimate for segment one (lowest, most pathological values of CSF $A\beta_{42}$) is the change in atrophy rate associated with a one unit increase of CSF $A\beta_{42}$. Note that all P -values are nonsignificant for segment one, indicating that there is no association between atrophy and $A\beta_{42}$ once levels of amyloid have become highly pathological. The estimate for the slope for segment 2 (transition period) is the sum of the estimates for segment 1 and 2. Similarly, the slope for segment 3 is the sum of all three estimates. In other words, for segments 2 and 3, the parameters are estimates of the change in slope, i.e. acceleration or stabilization, relative to the prior segment. A negative parameter estimate for segment 3 indicates an acceleration of atrophy as CSF $A\beta_{42}$ levels decrease from high levels to the transition period. A positive estimate for segment 2 indicates a stabilization of atrophy rates as subjects move from the transition period to low levels of CSF $A\beta_{42}$. Twelve regions demonstrated significant stabilization (segment 2 in Table 2), but became only marginally significant after FDR correction. All regions in Table 2 show negative estimates for segment 3 and positive estimates for segment 2.

Models using the binary parameterization of CSF $A\beta_{42}$ were compared with the spline models using likelihood ratio tests and AIC. The spline model had a lower AIC and was significantly better fitting for the hippocampus ($P = .03$), inferior temporal lobe ($P = .05$), entorhinal cortex ($P = .05$), cuneus ($P < .01$), putamen ($P = .05$), and the brainstem ($P = .05$). The spline model had a lower AIC and showed some evidence of a better fit according to a likelihood ratio test for the parahippocampus, middle temporal gyrus, banks of the superior temporal sulcus (bankssts), thalamus, precentral, postcentral, midposterior corpus callosum, and the central corpus callosum ($P < .10$). The binary form of CSF $A\beta_{42}$ did not fit any of the regions significantly better than the spline model, although it was a marginally better fit for the precuneus ($P = .10$, smaller AIC for the binary model). None of the other regions differed in fit ($P > .10$).

Fig. 2 shows the ordering of the transition periods with respect to the left-hand, or normal, side of the period. Regions toward the top of the figure begin their transition earlier. A red circle on the left side indicates significant acceleration (or stabilization if on the right), $P < .05$. A yellow

Table 2
Slope estimates and *P*-values for spline segments by region in MCI and control subjects

Region	Segment 1: 50–Knot ₁			Segment 2: Knot ₁ –Knot ₂		Segment 3: Knot ₂ –300		
	Knot ₁	Slope	<i>P</i>	ΔSlope	<i>P</i> (p _{FDR})	Knot ₂	ΔSlope	<i>P</i> (p _{FDR})
Insula	127	−0.17	.50	0.55	0.05 (.18)	236	−0.71	.001 (.02)
Inferior temporal	132	−0.81	.28	2.51	0.007 (.09)	212	−1.91	.001 (.02)
Temporal pole	135	−0.17	.40	0.60	0.018 (.12)	222	−0.54	.001 (.02)
Hippocampus	132	−0.14	.46	0.63	0.008 (.09)	214	−0.61	.002 (.02)
Middle temporal	134	−0.73	.28	2.47	0.006 (.08)	210	−1.70	.005 (.05)
Entorhinal	138	−0.15	.36	0.55	0.01 (.10)	208	−0.37	.006 (.05)
Fusiform	130	−0.25	.71	1.54	0.06 (.18)	213	−1.31	.01 (.08)
Isthmus cingulate	132	−0.05	.63	0.26	0.06 (0.18)	208	−0.24	.01 (.08)
Cuneus	163	−0.10	.08	1.04	0.02 (.12)	175	−1.00	.016 (.08)
Amygdala	158	0.00	>.99	0.13	0.03 (.16)	221	−0.15	.017 (.08)
Superior parietal	170	−0.50	.24	2.91	0.03 (.16)	193	−2.45	.04 (.16)
Superior temporal	138	−0.03	.94	0.90	0.10 (.26)	211	−0.79	.04 (.16)
Precuneus	149	−0.15	.59	0.77	0.06 (.18)	220	−0.67	.05 (.19)
Parahippocampus	142	−0.12	.28	0.47	0.007 (.09)	203	−0.27	.055 (.19)
Pars opercularis	167	−0.07	.34	0.71	0.06 (.18)	181	−0.67	.07 (.20)
Brainstem	125	−0.13	.56	0.26	0.29 (.44)	218	−0.41	.07 (.20)
Supramarginal	170	−0.28	.19	1.93	0.04 (.18)	188	−1.52	.08 (.20)
Caudate	168	−0.02	.80	0.27	0.21 (.37)	222	−0.46	.08 (.20)
Putamen	154	0.01	.89	0.15	0.22 (.37)	227	−0.29	.09 (.21)
Pars triangularis	170	−0.10	.14	0.49	0.07 (0.18)	191	−0.39	.09 (.21)
Bankssts	135	−0.10	.37	0.32	0.04 (.18)	202	−0.18	.095 (.21)
Posterior cingulate	125	−0.04	.78	0.23	0.22 (.37)	228	−0.23	.099 (.21)

circle indicates marginally significant acceleration/stabilization, $P < .10$.

In the MCI group alone, the hippocampus, middle temporal gyrus, banks of the superior temporal sulcus, rostral anterior cingulate, cuneus, insula, and brainstem showed marginally significant ($P < .10$) acceleration (significant for the hippocampus and middle temporal lobe, $P < .05$), while the hippocampus, banks of the superior temporal sulcus, rostral anterior cingulate, and middle temporal gyrus all showed significant stabilization of rates. The cuneus showed marginally significant stabilization ($P < .10$). In controls, the amygdala, cuneus and caudate showed marginally significant points of acceleration. Only the cuneus stabilized with marginal significance (data not shown).

4. Discussion

The findings of this analysis were (1) the trilinear spline model provided significantly improved error reduction compared with the binary parameterization for several brain regions, and in no instance did the binary parameterization provide a significantly better fit than the trilinear spline model, (2) the periods of atrophy acceleration are evident in several regions over the span of CSF A β accumulation, (3) the start of these acceleration periods vary by brain region, and (4) trilinear spline modeling demonstrates that some brain regions have accelerated atrophy well before subjects cross the threshold defining amyloid positivity in preclinical AD.

The first finding was that modeling of CSF A β_{42} via splines results in better fitting models with more predictive accuracy compared with the dichotomous model. The spline

model estimates of acceleration and stabilization of atrophy are consistent with local regression estimates, but spline models also provide estimates of transition points. The spline models also appear less prone to overfitting at the boundaries of the data, i.e. the amygdala in Fig. 1. The increased predictive ability of the trilinear model over the dichotomous model was most clearly seen in regions in the temporal and parietal lobes where transition periods were most significant.

Aside from a methodological improvement in statistical modeling, the important biological finding of this work is that regions with distinct periods of accelerated volume loss show signs of atrophy well before the CSF A β_{42} 192 ng/L threshold. That is, subjects with CSF A β_{42} greater than 192 ng/L are not considered to have “preclinical AD” by current convention. Nevertheless, the results in Fig. 2 clearly show that the insula, most of the temporal lobe, and much of the parietal lobe fit the profile for a sigmoid-like curve with the evidence of acceleration starting at CSF A β_{42} levels between 210 and 225 ng/L. The stabilization of rates appears to begin near CSF A β_{42} 130 ng/L for most temporal lobe regions. When using a dichotomous model, subjects approaching the threshold for A β positivity are included in the A β negative group, whereas the trilinear model demonstrates that they are transitioning to A β +. Combining these transitioning subjects with subjects who will remain A β − biases the association of A β_{42} with the response in the A β − group toward the A β + group, reducing group differences and the power to detect the effect of A β_{42} on other aspects of AD pathology, including brain atrophy. Further categorization of subjects into incident A β + or transitioning A β groups can be seen in recent research [28,29].

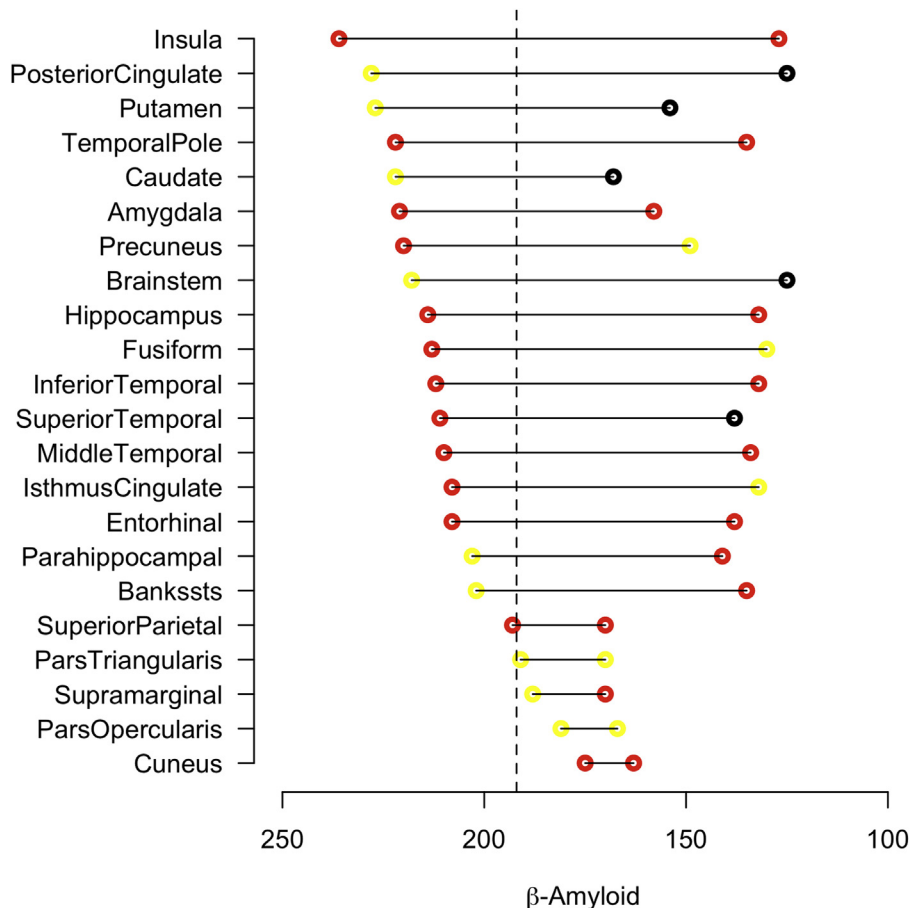


Fig. 2. Regions ordered by acceleration and stabilization points.

The finding of early Aβ-related atrophy in temporal and parietal lobes and the cingulate gyrus agrees with previous reports [8–12]. Several regions, including the insula, posterior cingulate, amygdala, putamen, and precuneus show early signs of atrophy even though they do not reach the magnitude of atrophy seen in much of the temporal lobe during the course of dementia due to AD. Fig. 2 shows that these regions may show signs of Aβ related atrophy before the hippocampus and entorhinal cortex which are generally thought to show neurodegeneration very early in AD. The length of the transition period with respect to Aβ is similar among the temporal lobe regions, but appears shorter in many of the parietal regions (Fig. 2). This extended acceleration period in the temporal lobe may contribute to atrophy rates reaching much higher levels compared with other lobes in the progression of AD, despite the possibility that brain atrophy may start to accelerate earlier in nontemporal regions.

Not all regions show a pattern of stability before a distinct transition period. In MCI subjects, there is a linear decline in the amygdala until an ostensible stabilization period near CSF Aβ₄₂ = 125 ng/L. If a point of acceleration exists for MCI subjects in the amygdala, it may have occurred beyond the upper range of CSF Aβ₄₂ in these subjects, suggesting an

early effect of Aβ on atrophy in the amygdala. A similar pattern occurred in the fusiform and parahippocampus of MCI subjects.

Control subjects do not have as steep a transition from high levels of CSF Aβ₄₂ to low levels even though a substantial number of control subjects are well beyond the clinical threshold for Aβ positivity. This suggests that an excess accumulation of Aβ alone does not necessarily result in an immediate increase in rates of atrophy and cognitive impairment. Latent factors, absent in controls, may contribute to an increased vulnerability of MCI subjects to the effects of Aβ. For example, the duration of exposure to Aβ pathology may be important for effects on brain atrophy, and may differ between controls and MCI. Commonly occurring copathologies such as Lewy Body (LB) and transactive response DNA binding protein 43 (TDP-43) pathology and cerebrovascular disease (CVD) may also influence the association of Aβ at any stage of preclinical or prodromal AD and will likely need to be taken into account and demonstrated in other cohorts [30–32].

One important implication for clinical trials attempting to treat Aβ-related atrophy and subsequent cognitive decline may be the recruitment of subjects with low enough levels of Aβ pathology for a drug to successfully change the course

of disease, but high enough for a placebo group to demonstrate an increased rate of atrophy, while also screening out subjects with LB, TDP-43 inclusions, or CVD to avoid confounds linked to these other pathologies when interpreting the response of individuals to a therapy that only targets A β pathology.

One limiting factor of this analysis is the sparsity of CSF A β_{42} data near the previously established clinical threshold 192 ng/L, precisely the interval of most interest. This sparsity will likely have some effect on the knot location selection, parameter estimates, and the power to detect significant acceleration in atrophy rate. By using CSF to measure A β pathology, we did not have information about sites of A β accumulation and could not account for variation in spatial deposition, another complicating factor likely to affect regional atrophy. Also, we report significant and marginally significant results. Marginally significant results should be interpreted with caution given the large number of regions tested, however, the common direction of the slopes across all AD-implicated regions provides some evidence of a more mild association rather than type I error.

In conclusion, we show that the relationship between CSF A β_{42} and regional brain atrophy rates may be parameterized by trilinear functions, providing an improved model of their association and may improve the characterization of A β pathology, compared with the usual binary classification. The results are consistent with the view that signs of brain atrophy develop before the decrease of CSF A β_{42} required in the current conventional definition of "preclinical AD".

Acknowledgments

Data collection and sharing for this project were funded by the Alzheimer's Disease Neuroimaging Initiative (ADNI) (National Institutes of Health Grant U01 AG024904). ADNI is funded by the National Institute on Aging, the National Institute of Biomedical Imaging and Bioengineering, and through generous contributions from the following: Alzheimer's Association; Alzheimer's Drug Discovery Foundation; BioClinica, Inc.; Biogen Idec Inc.; Bristol-Myers Squibb Company; Eisai Inc.; Elan Pharmaceuticals, Inc.; Eli Lilly and Company; F. Hoffmann-La Roche Ltd and its affiliated company Genentech, Inc.; GE Healthcare; Innogenetics, N.V.; IXICO Ltd.; Janssen Alzheimer Immunotherapy Research & Development, LLC.; Johnson & Johnson Pharmaceutical Research & Development LLC.; Medpace, Inc.; Merck & Co., Inc.; Meso Scale Diagnostics, LLC.; NeuroRx Research; Novartis Pharmaceuticals Corporation; Pfizer Inc.; Piramal Imaging; Servier; Synarc Inc.; and Takeda Pharmaceutical Company. The Canadian Institutes of Health Research is providing funds to support ADNI clinical sites in Canada. Private sector contributions are facilitated by the Foundation for the National Institutes of Health (www.fnih.org). The grantee organization is the Northern California Institute for Research and Education, and the study is coordinated by the Alzheimer's Disease

Cooperative Study at the University of California, San Diego. ADNI data are disseminated by the Laboratory for Neuro Imaging at the University of Southern California. This research was also supported by National Institutes of Health (NIH) grants P30 AG010129 and K01 AG030514.

Disclosure Statement: PSI and NM report no conflicts of interest. MCD was a consultant for Bristol-Myers Squibb. PSA serves on a scientific advisory board for NeuroPhase; has served as a consultant to Elan, Wyeth, Eisai, Schering-Plough, Bristol-Myers Squibb, Eli Lilly and Company, NeuroPhase, Merck, Roche, Amgen, Genentech, Abbott, Pfizer, Novartis, Bayer, Astellas, Dainippon, Biomarin, Solvay, Otsuka, Daiichi, AstraZeneca, Janssen, Medivation, Ichor, Toyama, Lundbeck, Biogen Idec, iPerian, Probiobdrug, Somaxon, Biotie, Cardeus, Anavex, Kyowa Hakko Kirin Pharma, Medtronic; and receives research support from Eli Lilly and Baxter, and the NIH [NIA U01-AG10483 (PI), NIA U01-AG024904 (Coordinating Center Director), NIA R01-AG030048 (PI), and R01-AG16381 (Co-I)]. RSM has financial support from NIMH R01 0977669 and NIMH K08 MH081065. CRJ has provided consulting services for Janssen Research & Development, LLC. He receives research funding from the National Institutes of Health (R01-AG011378, R01-AG041851, R01-AG037551, U01-HL096917, U01-AG032438, U01-AG024904), and the Alexander Family Alzheimer's Disease Research Professorship of the Mayo Foundation. LMS previously was consultant for Innogenetics and collaborates on quality assessment activities as part of the Alzheimer's Disease Neuroimaging Initiative; and serves as a consultant to Eli Lilly and Janssen AI R & D on biomarker studies. JQT may accrue revenue in the future on patents submitted by the University of Pennsylvania, wherein he is the co-inventor and he received revenue from the sale of Avid to Eli Lilly as the co-inventor on imaging-related patents submitted by the University of Pennsylvania; and is the William Maul Measey-Truman G Schnabel, Jr, MD Professor of Geriatric Medicine and Gerontology. MWW has been on scientific advisory boards for Pfizer and BOLT International; has been consultant for Pfizer Inc, Janssen, KLJ Associates, Easton Associates, Harvard University, in Thought, INC Research, Inc, University of California, Los Angeles, Alzheimer's Drug Discovery Foundation and Sanofi-Aventis Groupe; has received funding for travel from Pfizer, ADPD meeting, Paul Sabatier University, Novartis, Tohoku University, MCI Group, France, Travel eDreams, Inc, Neuroscience School of Advanced Studies (NSAS), Danone Trading, BV, CTAD ANT Congres; serves as an associated editor of *Alzheimer's & Dementia*; has received honoraria from Pfizer, Tohoku University, and Danone Trading BV; has research support from Merck, Avid, DOD and VA; and has stock options in Synarc and Elan.

Supplementary data

Supplementary data related to this article can be found at <http://dx.doi.org/10.1016/j.jalz.2014.11.002>.

RESEARCH IN CONTEXT

1. Systematic review: To identify all relevant research in the literature pertaining to our topic, we searched for papers referencing structural imaging in Alzheimer's disease and mild cognitive impairment, amyloid imaging, cerebrospinal fluid (CSF) biomarkers, brain atrophy, and statistical methods applied to longitudinal imaging studies including nonlinear and local regression, splines, trilinear models, and mixed-effects regression. Our authors, with expertise in imaging, CSF biomarkers, and statistics, reviewed and added to the citations to ensure completeness.
2. Interpretation: Our results demonstrate a statistical method that improves the characterization of the relationship between amyloid beta (A β) and atrophy compared with the most commonly used method in the literature. Our method is more powerful and offers a temporal ordering of the acceleration of atrophy of individual brain regions. This information will help facilitate the design of clinical trials aimed at treating amyloid pathology.
3. Future directions: Studies focused on subjects transitioning from A β negative to A β positive in a longitudinal setting will be required to more precisely estimate the evolution of regional atrophy.

References

- [1] Braak H, Braak E. Neuropathological staging of Alzheimer-related changes. *Acta Neuropathol* 1991;82:239–59.
- [2] Petersen RC, Roberts RO, Knopman DS, Boeve BF, Geda YE, Ivnik RJ, et al. Mild cognitive impairment: ten years later. *Arch Neurol* 2009;66:1447–55.
- [3] Hardy J, Selkoe DJ. The amyloid hypothesis of Alzheimer's disease: progress and problems on the road to therapeutics. *Science* 2002; 297:353–6.
- [4] Bateman RJ, Xiong C, Benzinger TL, Fagan AM, Goate A, Fox N, et al. Clinical and biomarker changes in dominantly inherited Alzheimer's disease. *N Engl J Med* 2012;367:795–804.
- [5] Jack CR Jr, Lowe VJ, Weigand SD, Wiste HJ, Senjem ML, Knopman DS, et al., Alzheimer's Disease Neuroimaging Initiative. Serial PIB and MRI in normal, mild cognitive impairment and Alzheimer's disease: implications for sequence of pathological events in Alzheimer's disease. *Brain* 2009; 132:1355–65.
- [6] Jack CR, Knopman DS, Jagust WJ, Shaw LM, Aisen PS, Weiner MW, et al. Hypothetical model of dynamic biomarkers of the Alzheimer's pathological cascade. *Lancet Neurol* 2010;9:119–28.
- [7] Rowe CC, Ellis KA, Rimajova M, Bourgeat P, Pike KE, Jones G, et al. Amyloid imaging results from the Australian Imaging, Biomarkers and Lifestyle (AIBL) study of aging. *Neurobiol Aging* 2010; 31:1275–83.
- [8] Chételat G, Villemagne VL, Villain N, Jones G, Ellis KA, Ames D, et al. Accelerated cortical atrophy in cognitively normal elderly with high β -amyloid deposition. *Neurology* 2012; 78:477–84.
- [9] Chételat G, Villemagne VL, Bourgeat P, Pike KE, Jones G, Ames D, et al. Relationship between atrophy and β -amyloid deposition in Alzheimer disease. *Ann Neurol* 2010;67:317–24.
- [10] Doré V, Villemagne VL, Bourgeat P, Frapp J, Acosta O, Chételat G, et al. Cross-sectional and longitudinal analysis of the relationship between a deposition, cortical thickness, and memory in cognitively unimpaired individuals and in Alzheimer disease. *JAMA Neurol* 2013; 70:903–11.
- [11] Tosun D, Schuff N, Mathis CA, Jagust W, Weiner MW. Spatial patterns of brain amyloid- β burden and atrophy rate associations in mild cognitive impairment. *Brain* 2011;134:1077–88.
- [12] Cash DM, Ridgway GR, Liang Y, Ryan NS, Kinnunen KM, Yeatman T, et al. The pattern of atrophy in familial Alzheimer disease volumetric MRI results from the DIAN study. *Neurology* 2013; 81:1425–33.
- [13] Toledo J, Xie S, Trojanowski J, Shaw L. Longitudinal change in CSF Tau and A β biomarkers for up to 48 months in ADNI. *Acta Neuropathol* 2013;126:1–12.
- [14] Villemagne VL, Burnham S, Bourgeat P, Brown B, Ellis KA, Salvado O, et al., Australian Imaging Biomarkers and Lifestyle (AIBL) Research Group. Amyloid β deposition, neurodegeneration, and cognitive decline in sporadic Alzheimer's disease: a prospective cohort study. *Lancet Neurol* 2013;12:357–67.
- [15] Jack CR Jr, Wiste HJ, Lesnick TG, Weigand SD, Knopman DS, Vemuri P, et al. Brain β -amyloid load approaches a plateau. *Neurology* 2013;80:890–6.
- [16] Bourgeat P, Chételat G, Villemagne VL, Frapp J, Raniga P, Pike K, et al. β -Amyloid burden in the temporal neocortex is related to hippocampal atrophy in elderly subjects without dementia. *Neurology* 2010; 74:121–7.
- [17] Shaw LM, Vanderstichele H, Knopik-Czajka M, Clark CM, Aisen PS, Petersen RC, et al. Cerebrospinal fluid biomarker signature in Alzheimer's disease neuroimaging initiative subjects. *Ann Neurol* 2009; 65:403–13.
- [18] Cleveland WS, Devlin S. Locally weighted regression: an approach to regression analysis by local fitting. *JASA* 1988; 83:596–610.
- [19] Hastie TJ, Tibshirani RJ. Generalized additive models. Boca Raton: CRC Press; 1990.
- [20] Schuff N, Tosun D, Insel PS, Chiang GC, Truran D, Aisen PS, et al. Nonlinear time course of brain volume loss in cognitively normal and impaired elders. *Neurobiol Aging* 2012; 33:845–55.
- [21] Davatzikos C, Xu F, An Y, Fan Y, Resnick SM. Longitudinal progression of Alzheimer's-like patterns of atrophy in normal older adults: the SPARE-AD index. *Brain* 2009;132:2026–35.
- [22] McDonald CR, McEvoy LK, Gharapetian L, Fennema-Notestine C, Hagler DJ, Holland A, et al. Regional rates of neocortical atrophy from normal aging to early Alzheimer disease. *Neurology* 2009; 73:457–65.
- [23] Brooks JO 3rd, Kraemer HC, Tanke ED, Yesavage JA. The methodology of studying decline in Alzheimer's disease. *J Am Geriatr Soc* 1993;41:623–8.
- [24] Olsson A, Vanderstichele H, Andreassen N, De Meyer G, Wallin A, Holmberg B, et al. Simultaneous measurement of beta-amyloid(1–42), total tau, and phosphorylated tau (Thr181) in cerebrospinal fluid by the xMAP technology. *Clin Chem* 2005;51:336–45.
- [25] Jack CR Jr, Bernstein MA, Fox NC, Thompson P, Alexander G, Harvey D, et al. The Alzheimer's Disease Neuroimaging Initiative (ADNI): MRI methods. *J Magn Reson Imaging* 2008; 27:685–91.
- [26] Davison AC, Hinkley DV. Bootstrap methods and their application. Cambridge, UK: Cambridge University Press; 1997.

- [27] Benjamini Y, Hochberg Y. Controlling the false discovery rate: a practical and powerful approach to multiple testing. *J R Statist Soc B* 1995; 57:289–300.
- [28] Jack CR, Wiste HJ, Weigand SD, Knopman DS, Lowe V, Vemuri P, et al. Amyloid-first and neurodegeneration-first profiles characterize incident amyloid PET positivity. *Neurology* 2013; 81:1732–40.
- [29] Mattsson N, Insel PS, Nosheny R, Tosun D, Trojanowski JQ, Shaw LM, et al. Emerging β -amyloid pathology and accelerated cortical atrophy. *JAMA neurol* 2014;71:725–34.
- [30] Toledo JB, Brettschneider J, Grossman M, Arnold SE, Hu WT, Xie SX, et al. CSF biomarkers cutoffs: the importance of coincident neuropathological diseases. *Acta Neuropathol* 2012;124:23–35.
- [31] Toledo JB, Arnold SE, Raible K, Brettschneider J, Xie SX, Grossman M, et al. Contribution of cerebrovascular disease in autopsy confirmed neurodegenerative disease cases in the National Alzheimer's Coordinating Centre. *Brain* 2013;136:2697–706.
- [32] Toledo JB, Cairn N, Da X, Chen K, Shaw LM, Davatzikos C, et al. Clinical and multimodal biomarker correlates of ADNI neuropathological findings. *Acta Neuropathol Commun* 2013;1:65.